SciEn

Proceedings of 7th International Conference on Mechanical, Industrial and Energy Engineering-Part I
22-24 December, 2022, Khulna, BANGLADESH

SciEn Conference Series: Engineering Vol. 1, 2025, pp 41-46 https://doi.org/10.38032/scse.2025.1.8

Scattering Directivity Pattern Analysis of Low-frequency Lamb Wave at Sub-surface Damage in Composite Laminates

M S Rabbi[1,*], *K Teramoto*[2], *H Ishibashi*[3], *T I Khan*[2]

[1] Department of Mechanical Engineering, Chittagong University of Engineering & Technology, Chattogram-4349, BANGLADESH

[2] Department of Advanced Technology Fusion, Saga University, 1 Honjo-machi, Saga, 840-8502, JAPAN

[3]Wakayama College, National Institute of Technology, Wakayama 644-0023, JAPAN

ABSTRACT

This article presents the scattering phenomena of the low-frequency zero order anti-symmetric (A_0) mode Lamb wave at a sub-surface defect in composite laminates. The variable angular amplitude distribution at the defect is one of the key factors affect damage detection algorithm development, toward unavailability of the analytical model of the scattered wave. In this research, the numerical study to investigate the reflection and transmission characteristics of A_0-mode Lamb wave at a subsurface defect is investigated. Cross-ply CFRP laminates with sub-surface damage of the various size of the defect were considered as the specimen. Each layer of the laminate considered as horizontally and vertically transversely isotropic material. Numerical simulation is carried out using explicit type software LS-DYNA. Low frequency Lamb wave of 30 kHz is excited by a sinusoidal toneburst. To calculate the Scattering Directivity Pattern (SDP), time dependent normal displacements are recorded. Numerical results are compared with the experimental study. This study shows that the fiber orientation of the outer laminae has a significant influence on the scattering characteristics and less impact on the size of the defect.

Keywords: A_0-mode Lamb wave, CFRP laminate, Scattering characteristics, Fiber direction.

1. Introduction

The necessity of the composite structures' health monitoring is widely recognized due to its reliability and low life-cycle cost. Lamb wave-based SHM technique becomes popular due to its sensitivity to the small defect (disbands and delaminations) in composite material [1-3]. In most cases, development of a damage detection technique depends on the perception of the scattering characteristics of Lamb wave in the defected object. Scattering phenomena of Lamb wave with different types of flaws have been interrogated by the numerous researchers [4-7]. The anisotropic properties of the composite material hinder to find out a proper mathematical model for scattering pattern prediction. Among various order of Lamb wave, the zero order modes (A_0 and S_0) have been extensively used for due to their availability at low frequency regime. Out-of-plane displacement of the fundamental order Lamb wave mode is depicted in Fig. 1.

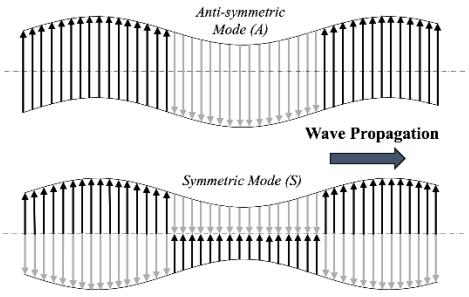

Fig. 1 Out-of-plane displacement of Antisymmetric (*A*) and Symmetric (*S*) mode Lamb wave

The exciting features of the A_0-mode Lamb wave compared to S_0-mode is relatively eased of generation. Moreover, it possesses shorter wavelength. In the last decades, plenty of investigations have been carried out through computational and experimental study to measure the scattering characteristics of Lamb wave [1, 8-11]. Gangwar et. al. examined the nonlinear interactions of A_0-mode Lamb wave with a through-width delamination GFRP laminate [12]. Munian et. al. interrogated the Lamb wave interaction with composite delamination [13]. It was found that the energy of the scattered wave due to the defect depends on the resonance properties of the sub-layup. The scattering coefficients of A_0-mode Lamb wave calculated by Haider et. al. for a plate with cracked stiffener [14]. A 3D FEM is presented to predict the Lamb wave at delaminations in Quasi-isotropic (QI) laminate by Pudipeddi et. al. [15]. They found that the scattering of propagating wave and their mode conversion phenomena depends upon the fiber orientation of the outer lamina, the defect size and location. Nonlinear Lamb waves scattering phenomena at delamination is addressed by Soleimanpour et. al [16]. They successfully predicted and observed the higher harmonics of Lamb wave through computational and experimental studies. An efficient numerical approach is proposed by Shen et. al [17] to observe the nonlinear scattering of Lamb wave at breathing cracks. The influence of oblique incident angle on scattering is investigated in their study.

Chiu et al. investigated the scattering phenomena by delamination at the edge of a QI composite laminate [18]. It was reported that the scattering behavior and amplitude significantly affected by flaw size to the wavelength ratio.

Most of the researchers carried out the experiments for the through-thickness cylindrical damage and for the delamination in composite laminate. Limited number of investigations are reported for the interaction of Lamb wave

*Corresponding Author Email Address: rabbi@cuet.ac.bd

at subsurface damage. This research discussed the scattering directivity pattern of the A_0-mode Lamb wave in low frequency regime at a subsurface defect in cross-ply laminate to study the influence of damage size.

Section 2 will mention the material details used in this study. Finite Element Modelling (FEM) and meshing for computational analysis is discussed in Section 3. Scattering Directivity Pattern generation for various samples are explained in Section 4. Conclusions are drawn in Section 5.

2. Materials

Carbon Fiber Reinforced Polymer (CFRP) is considered as the composite laminate in this study to analysis the scattering phenomenon at the subsurface defect. The essential component of such laminate is carbon strand (7-15 μm in width) as reinforcement and usually epoxy-resin as matrix. A 8-layered ($[0/90]_{2S}$) composite laminate with subsurface cylindrical defect is considered. Schematic of the fiber directional lay-up is depicted in Fig. 2. The engineering constants of 0° layer is determined using micromechanical modelling [19] and corresponding stiffness matrix is given in Table 1:

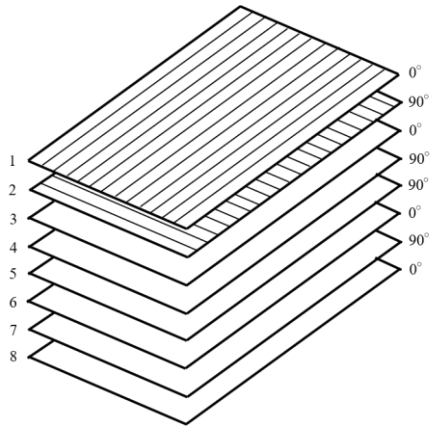

Fig. 2 Schematic of the composite laminate lay-up considered in this study.

Table 1 Stiffness matrix component for horizontally transverse isotropic material (unidirectional lamina with 0° fiber direction).

Component	Value (GPa)
C_{I1}	96.0
$C_{22} = C_{33}$	9.60
$C_{12} = C_{21}$	3.60
$C_{23} = C_{32}$	7.01
$C_{13} = C_{31}$	3.60
C_{44}	1.29
$C_{55} = C_{66}$	3.30

The density of each layer is considered 1500 kg/m^3. Fig. 3 depicted the dispersion curve of Lamb wave for such material. From the analytical study, wavelengths are found 7.36 mm and 5.60 mm in the fiber direction and perpendicular to the fiber direction respectively for 0° unidirectional lamina. The next section illustrated the details of the computational study.

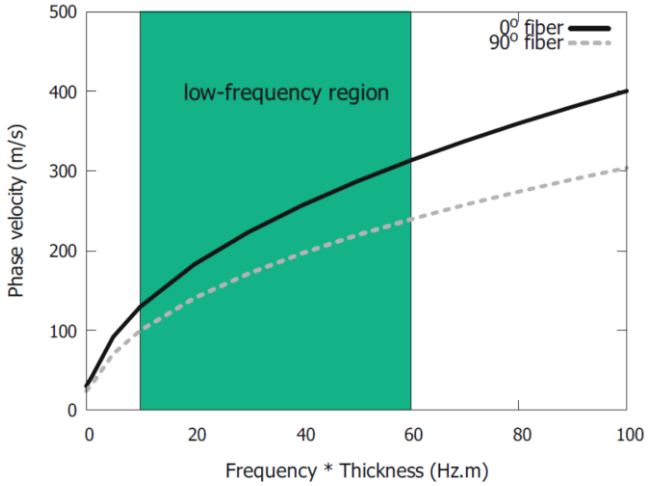

Fig. 3 Phase velocity dispersion curves for the considered value of the unidirectional laminate.

3. Computational Analysis

The computational analysis is conducted to measure the zero-order antisymmetric mode Lamb wave propagating through the cross-ply composite laminate. 3D model generation and numerical simulations are done in LS-DYNA [20]. Spatial dimension of the model is considered 100 mm × 100 mm whereas the thickness of the laminate is 1 mm. To predict the wave propagation perfectly, proper number of nodes per wavelength are required. A fine mesh of dimension 0.1 mm × 0.1 mm is considered. It ensures that at least 20 nodes are available per wavelength [21]. Each layer was designed using reduced integration solid brick with homogeneous and orthotropic material assumptions. Stiffness-weighted damping ratio of 0.015% was used to simulate the damping effect of the laminate [11]. Validation of the model is done by exciting sinusoidal wave with a frequency of 30, 40, and 50 kHz, respectively in a $[0]_8$ flawless laminate. In the surface coordinate (x-y) system, mid-section of the plate in the thickness direction is chosen to gather data. At the mid-section, zero order symmetric (S_0) and shear-horizontal (SH_0) mode have zero out-of-plane displacement ensures the availability of only the A_0-mode Lamb wave. It is noteworthy that, at this low frequency only zero-order modes could be exists. It is found good agreement with the theoretical values with the numerical values [Fig. 4]. To run the experiment in defected plate, 30 kHz mono-cycle tone burst nodal out-of-plane displacement applied to the L-end surface nodes. Fig. 5 Shows the schematic of the model. Elements are removed from the geometry to generate the defect upto the 7th layer from the bottom, i.e. depth of the damage is 0.95 mm with various diameter (1 mm, 0.75 mm, and 0.50 mm). Fig. 6 depicts the meshing and the cross section of the subsurface defect used in FE simulation. Fiber direction of each layer maintained as per Fig. 2. Fig. 7 illustrates the radial dependency of the phase velocity for cross-ply flawless laminate. Each value of the phase velocity is normalized by its maximum value. For satisfying the finite difference computational study, the time step is approximately 100 ns was taken [22]. After excitation, Lamb wave strikes at the boundary of the defect, reflection and transmission immediately occurred throughout the entire defected area (Fig. 8). Fig. 9 illustrates the decaying characteristics of the amplitude as a function of distance at the surroundings of the subsurface defect along the fiber direction for the intact and defected plate.

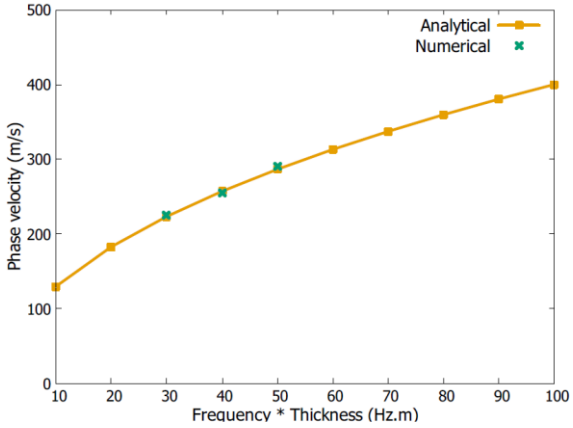

Fig. 4 Comparison of the phase velocity dispersion curve for HTI material.

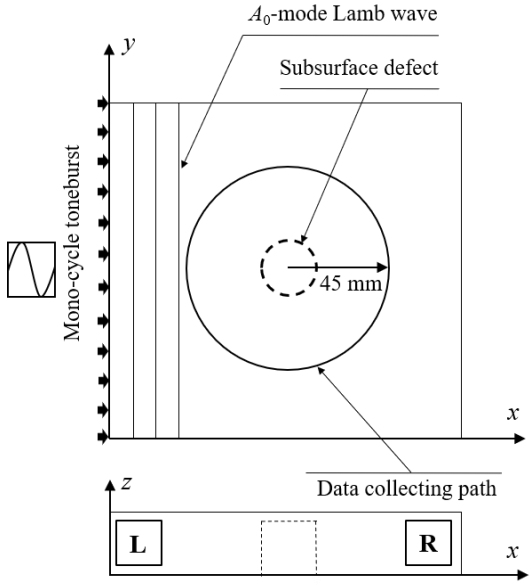

Fig. 5 Schematic diagram of the FE simulation.

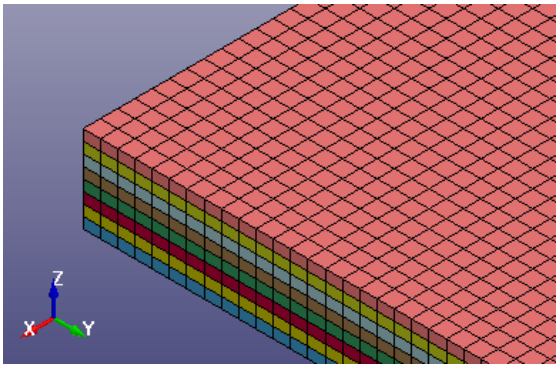

(a)

(b)

Fig. 6 (a) FEM meshing of flawless region (b) Cross-section of the subsurface defect.

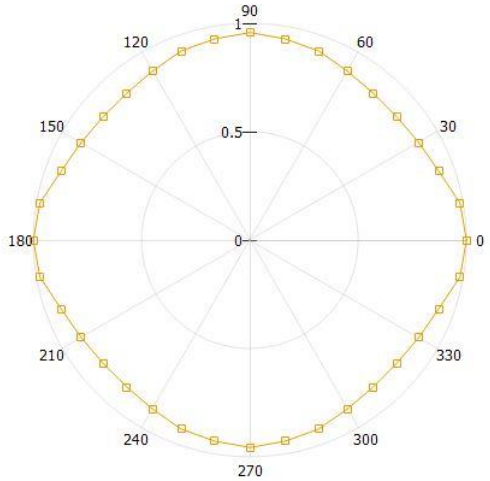

Fig. 7 Angular dependence of the phase velocity of $[0/90]_{2S}$ laminate (Measured values are normalized with the maximum value).

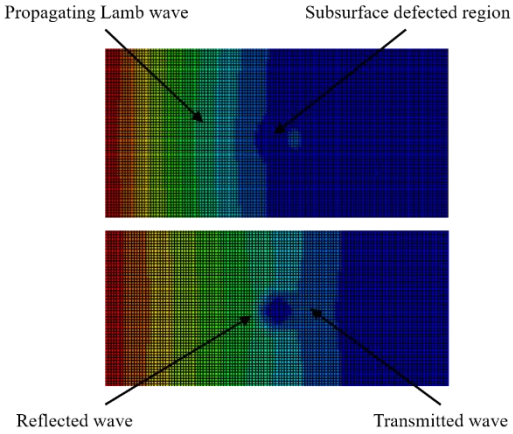

Fig. 8 Snapshots of the FE modelled wave propagation profile at the time of (up) striking at the defect and (down) scattered accordingly.

4. Scattering Directivity Pattern

Scattering Directivity Pattern (SDP) can be termed as the directional dependability of the scattered wave field due to anisotropy of the composite material. In this study, effect of the damage size on the scattering pattern is analyzed. Using the baseline subtraction technique, additional out-of-plane displacement is calculated. To carried out the process, a couple of numerical simulations were conducted for each case.

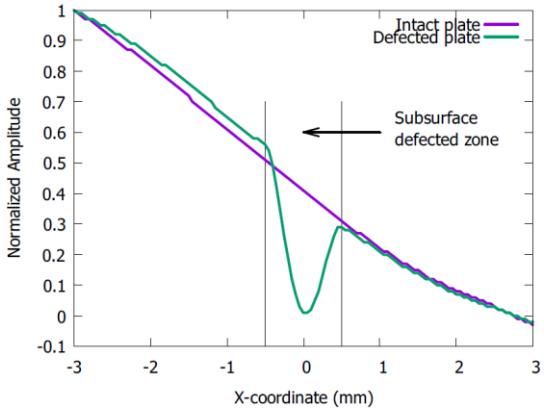

Fig. 9 Amplitude (normalized) is decaying as a function of wave propagation distance in the cross-ply laminate in the

vicinity (within 3 mm in both side from the center) of the defect.

One for the intact plate and another from defected plate, considering other factors remain identical. The data is collected at a circular path, 45 mm radius from the center of the plate, illustrated in Fig. 5. This ensures perfect capturing of the scattered wave by avoiding the evanescent wave. The scattered waves were gathered from 36 monitoring locations with a 10º step increment. Calculated SDP for various size of the defect is depicted in Fig. 10.

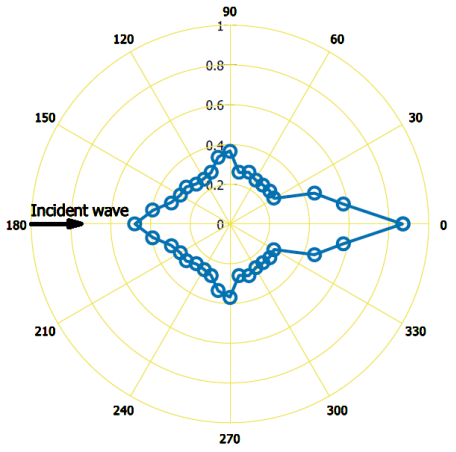

(a)

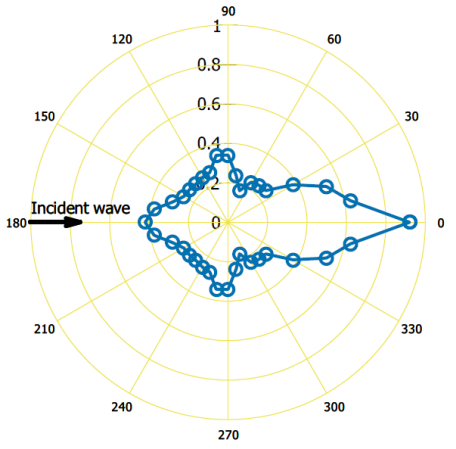

(b)

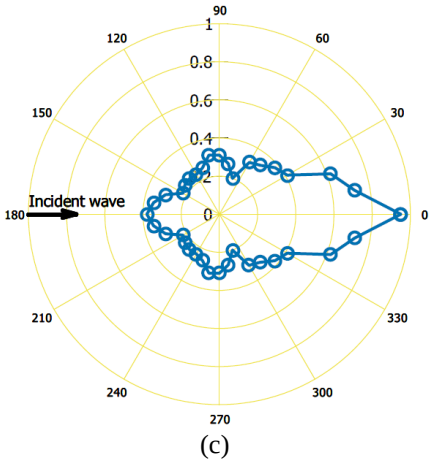

(c)

Fig. 10 Scattering Directivity Pattern (SDP) of the $[0/90]_{2S}$ laminate for (a) 1 mm defect, (b) 0.75 mm defect, and (c) 0.50 mm defect.

Though the shape of the SDPs looks alike for each case, the variation at every radial direction is so significant. The pattern looks symmetric in three cases. It is due to the symmetric lay-up of the considered plate. Fig. 11 illustrates the variations of amplitude for various defect size. It can be seen that, due to the less reflection in 0.50 mm defect, amplitude is higher in the 0° direction, i.e. outer layer fiber direction is dominant. Furthermore, due to the less reflection, the backward out-of-plane displacement is lower for the small size defect. It is observed that the scattering amplitude is not so significant for the angles $30° \leq \theta \leq 60°$ and $120° \leq \theta \leq 150°$. From this observation, it can be said that, the scattering characteristics depends upon the fiber orientation of the layer rather than the damage size. Such significant insight of the reflection characteristic of the low-frequency zero mode antisymmetric Lamb wave can be used to develop a damage detection technique in composite laminate.

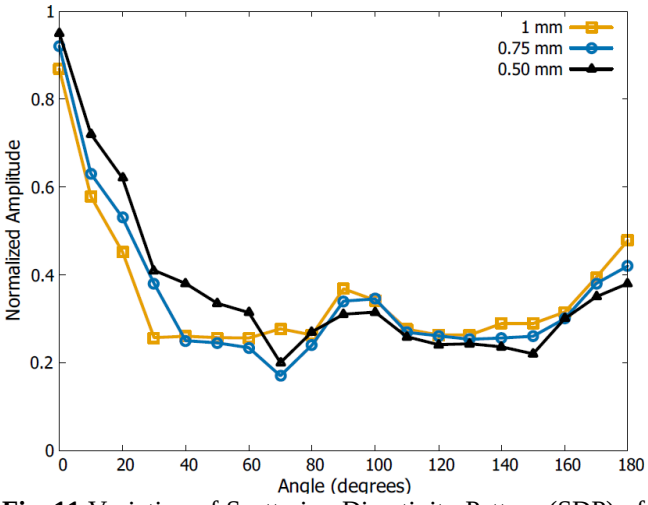

Fig. 11 Variation of Scattering Directivity Pattern (SDP) of the $[0/90]_{2S}$ laminate.

5. Experimental Investigation

To validate the numerical study, experimental investigation is carried out. Fig. 12 depicts the setup used in this study. Langevin transmitter is attached at

the center of the plate to irradiate the cylindrical wave. Michelson interferometric probe with capability of capturing amplitude upto 0.08nm is used to record the amplitudes from the spatial surface. Numerical and experimental wave frontal profiles are compared in Fig. 13. It can be seen that, except the 30° direction, the error lies within the 2% of the reference value. Subsurface defect of 1 mm in diameter is generated by engraving the material by center punch from the bottom surface of the laminate, 2 mm in thickness [Fig. 14]. From the observed experimental data, SDP is calculated and depicted in Fig. 15. Discrepancies are found in experimental data in comparing with the numerical values. Fig. 16 illustrates the absolute error percentage between these two sets of values. Though in both cases, fiber direction of the outer lamina dominates the scattering pattern, the anomalies can be occurred due to the rough surface of the engraved cylindrical hole. It can be observed that along with the outer lamina fiber direction the percentage of error relatively small. It might be occurred due to the overall dominance of the 0° lamina in wave propagation (both incident and scattered). Furthermore, the rough surface around the engraved blind hole (Fig. 14) might affect the scattering amplitude. Moreover, the vibration occurred at the center of the plate should have been dissipated at the boundary. Insufficient amount of damping material might cause the difficulties in capturing amplitudes perfectly.

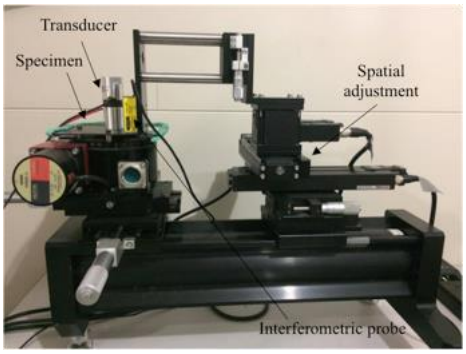

Fig. 12 Experimental setup used in this study depicting the transducer, specimen, and the vibrometer.

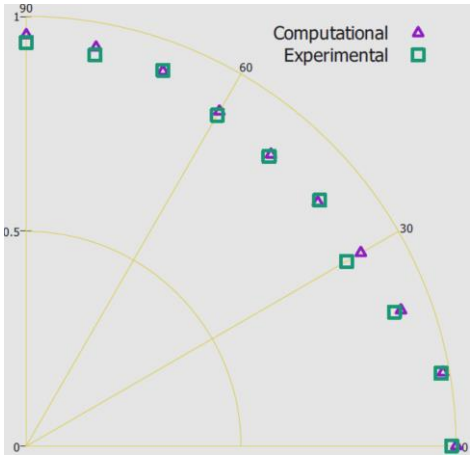

Fig. 13 Wave frontal profile for the 8-ply $[0/90]_{4S}$ composite laminate.

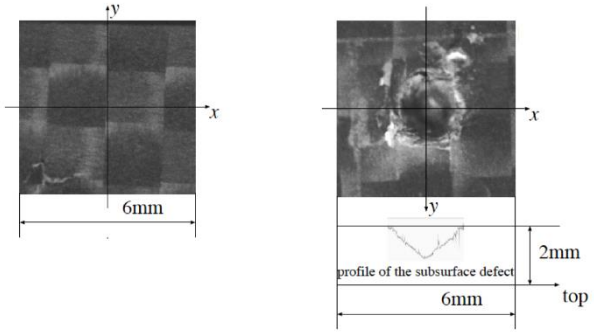

Fig. 14 Photograph of the subsurface defected composite laminate.

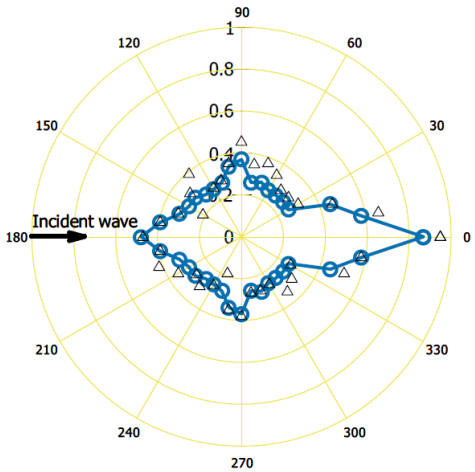

Fig. 15 SDP of A_0-mode Lamb wave in $[0/90]_{2S}$ laminate (empty circle: computational value, empty triangle: experimental value).

Fig. 16 depicts that except the error occurred at 130° and 210° nodal position, for other monitoring position, the error occurred within 10% of the reference value. Moreover, unlike the numerical outcome, it is found that the scattering values are not symmetrical with respect to the horizontal axis. This meaningful insight can be used to develop mathematical model to predict the scattered wave in subsurface defected composite laminate.

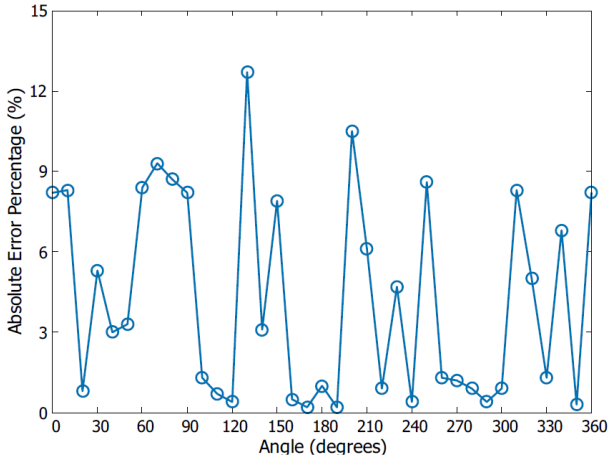

Fig. 16 Absolute error percentage of captured experimental value than numerical value.

5. Conclusion

The analysis of the Scattering Directivity Pattern (SDP) of the zero Antisymmetric mode Lamb wave in composite laminate is presented in this paper. Effect of the subsurface defect with various size on the SDP is investigated. Dispersion curve of the considered material is calculated theoretically and solved using MATLAB program for low-frequency. Computational study conducted using the explicit software LS-DYNA. Finite Element Modeling (FEM) was carried out for proper mesh size (0.1 mm × 0.1 mm) with respect to the Lamb wave wavelength. This condition ensures the perfect prediction of the considered wave within the model. Out-of-plane displacement from the top surface of the model is captured for the intact and defected plate. It is noteworthy that the wave propagation profile follows the fiber direction of the out layer (0°). The baseline subtraction method was used to calculate the SDP. Experimental study is carried out to compare the outcome of the numerical simulation. It is found that fiber orientation made significant impact on scattering phenomena rather the subsurface damage size.

7. Acknowledgement

This research was supported by The Ministry of Education, Culture, Sports, Science and Technology (MEXT) scholarship, the Government of Japan.

References

[1] Guo, N, Cawley, P., The interaction of Lamb waves with delaminations in composite laminates, *The Journal of the Acoustical Society of America*, vol. 94(4), pp. 2240-2246, 1993.

[2] Boller, C., Next generation structural health monitoring and its integration into aircraft design, *Int. J. Syst. Sci.*, vol. 31, pp.1333–1349, 2000.

[3] Rabbi, M. S., Teramoto, K., Ishibashi, H., Roshid,

M.M., Imaging of Sub-surface Defect in CFRP Laminate using A0-mode Lamb wave: Analytical, Numerical and Experimental studies, *Ultrasonics*, vol. 167, p.106849, 2022.

[4] Cegla, F. B., Rohde, A., Veidt, M., Analytical prediction and experimental measurement for mode conversion and scattering of plate waves at non-symmetric circular blind holes in isotropic plates. *Wave Motion*, vol. 45(3), pp.162-177, 2008.

[5] Lowe, M. J., Cawley, P., Kao, J. Y., Diligent, O., The low frequency reflection characteristics of the fundamental antisymmetric Lamb wave a0 from a rectangular notch in a plate, *The Journal of the Acoustical Society of America*, vol. 112(6), pp.2612-2622, 2002.

[6] Moreau, L., Castaings, M., The use of an orthogonality relation for reducing the size of finite element models for 3D guided waves scattering problems, *Ultrasonics*, vol. 48(5), pp.357-366, 2008.

[7] Alleyne, D. N., Cawley, P., The interaction of Lamb waves with defects, *IEEE transactions on ultrasonics, ferroelectrics, and frequency control*, vol. 39(3), pp.381-397, 1992.

[8] Hayashi, T., Kawashima, K., Multiple reflections of Lamb waves at a delamination, *Ultrasonics*, vol. 40(1-8), pp.193-197, 2002.

[9] McKeon, J. C. P., Hinders, M. K., Lamb wave scattering from a through thickness hole, *Journal of Sound and Vibration*, vol. 224(5), pp.843-862, 1999

[10] Ng. C. T., Veidt, M., Rose, L.R. F., Wang, C. H., Analytical and finite element prediction of Lamb wave scattering at delaminations in quasi-isotropic composite laminates, *Journal of Sound and Vibration*, vol. 331, pp. 4870-4883, 2012.

[11] Veidt, M., Ng, C. T., Influence of stacking sequence on scattering characteristics of the fundamental anti-symmetric Lamb wave at through holes in composite laminates, *Journal of Acoustical Society of America*, vol. 129(3) pp.1280-1287, 2011

[12] Gangwar, A. S., Agrawal, Y., Joglekar, D. M., Nonlinear interactions of lamb waves with a delamination in composite laminates, *Journal of Nondestructive Evaluation, Diagnostics and Prognostics of Engineering Systems*, vol. 4(3), 2021.

[13] Munian, R. K., Mahapatra, D. R., Gopalakrishnan, S. Lamb wave interaction with composite delamination, *Composite Structures*, vol. 206, pp.484-498, 2018

[14] Haider, M. F., Bhuiyan, M. Y., Poddar, B., Lin, B., Giurgiutiu, V., Analytical and experimental investigation of the interaction of Lamb waves in a stiffened aluminum plate with a horizontal crack at the root of the stiffener, *Journal of Sound and Vibration*, vol. *431*, pp.212-225, 2018

[15] Pudipeddi, G. T., Ng, C. T., Kotousov, A., Mode conversion and scattering of Lamb waves at delaminations in composite laminates, *Journal of Aerospace Engineering*, vol. 32(5), p.04019067, 2019

[16] Soleimanpour, R., Ng, C. T., Scattering analysis of nonlinear Lamb waves at delaminations in composite laminates, *Journal of Vibration and Control*, No. 1077546321990145, 2021

[17] Shen, Y., Cesnik, C. E., Nonlinear scattering and mode conversion of Lamb waves at breathing cracks: An efficient numerical approach, *Ultrasonics*, vol. 94, pp.202-217, 2019

[18] Chiu, W. K., Rose, L. R. F., Nadarajah, N., Scattering of the fundamental anti-symmetric Lamb wave by a mid-plane edge delamination in a fiber-composite laminate, *Procedia Engineering*, vol. 188, pp.317-324, 2017

[19] Chamis, C. C., Mechanics of composite materials: past, present, and future, *Journal of Composites, Technology and Research*, vol. 11(1), pp.3-14, 1989

[20] Manual LD, Volume I. Version 971, Livermore Software Technology Corporation, 2007

[21] Alleyne, D. N., Cawley, P., The interaction of Lamb waves with defects, *IEEE transactions on ultrasonics, ferroelectrics, and frequency control*, vol. 39(3), pp.381-397, 1992

[22] Courant, R., Friedrichs, K., Lewy, H., On the partial difference equations of mathematical physics. *IBM journal of Research and Development*, vol. 11(2), pp.215-234, 1967.